Interleaver Technology: Comparisons and Applications Requirements

S. Cao, J. Chen, J. N. Damask, C. R. Doerr, L. Guiziou, G. Harvey, Y. Hibino, H. Li, S. Suzuki, K.-Y. Wu, and P. Xie

***Abstract*—An overview of interleaver technologies is presented, based on the workshop held at the Optical Fiber Communications Conference, March 23, 2003. The requirements for and several realizations of interleaver filters are detailed.**

***Index Terms*—Optical components, optical filters, wavelength division multiplexing (WDM).**

I. Introduction

On March 23, 2003, a workshop on interleaver technologies was held as part of the Optical Fiber Communications Workshop Series. The authors of this paper were the organizers of and speakers at the workshop, and this contribution is intended to capture an overview of the field as it is currently practiced. The speakers were invited based on their original contributions to the field.

An interleaver is a periodic optical filter that combines or separates a comb of dense wavelength-division multiplexed (DWDM) signals. The periodic nature of the interleaver filter reduces the number of Fourier components required for a flat passband and high-isolation rejection band. This is in contrast to single-channel add/drop filters that synthesize a single narrow-band filter over a wide rejection band. Because the interleaver requires fewer Fourier components, the same flat top, sharp edge response of a higher-order narrow-band filter can be realized with only a few sections.

As a functional block, interleavers come in many varieties. The original design separates (or combines) even channels from odd channels across a DWDM comb, Fig. 1(a). This is denoted a 1:2 interleaver. The logical extension is the periodic separation of one in every 2^N channels, such as the 1:4 function illustrated in Fig. 1(b). A different variation is the banded interleaver, Fig. 1(c), where bands of channels are periodically separated. This is a more difficult filter to make because the filter roll-off must be steeper in relation to the filter period. Finally, in contrast with the previous three filters, the asymmetric filter periodically separates one channel in N, Fig. 1(d).

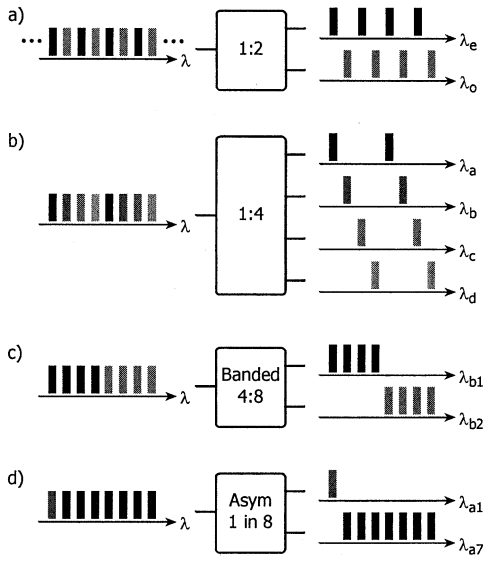

Fig. 1. Interleaver functional types. All filter functions are periodic in frequency and are reciprocal. (a) Original interleaver: even and odd channels are separated onto two different ports. (b) Separation of channels out to 1:4 or higher. (c) Banded interleaver, separates even and odd bands of channels. More difficult than 1:2 interleaver because of higher filter roll-off. (d) Asymmetric interleaver separates one channel in N.

The filter function of an interleaver and its period are separable. Interleavers have been demonstrated that resolve a comb of DWDM frequencies on 100-, 50-, 25-, and 12.5-GHz centers. The period is governed by the free-spectral range of the core elements, where narrower channel spacing is achieved by a longer optical path.

There are many specifications and design goals that are common to interleavers regardless of the particular technology used for implementation. On a per-channel level for a representative 1:2 interleaver, the amplitude spectrum at either of the two output ports has a passband and a stopband, Fig. 2(a). The design goals for the passband are a wide, flat (or nearly flat) top with minimum insertion loss (IL) and rapid rolloff on the band edges. The chromatic dispersion across the passband is to be minimized. The stopband must provide high extinction across the passband of the alternate port. This usually requires a tradeoff between maximum extinction and stopband width. For

Manuscript received June 25, 2003; revised September 15, 2003.

S. Cao is with Arasor Corporation, Fremont, CA 94538 USA (e-mail: scao@arasor.net).

J. Chen is with the Institute of Electro-Optical Engineering, National Chiao Tung University, Hsinchu, Taiwan (e-mail: jchen@faculty.nctu.edu.tw).

J. N. Damask is at 201 West 89th St., Apt 3C, New York, NY 10024 USA (e-mail: damask@alum.mit.edu).

C. R. Doerr is with Bell Laboratories, Lucent Technologies, Holmdel, NJ 07733 USA (e-mail: crdoerr@lucent.com).

L. Guiziou is with OpsiTech, S.A., Grenoble, France (e-mail: laurent.guiziou@opsitech.com).

G. Harvey and H. Li are with Tyco Telecommunications, Eatontown, NJ 07724 USA (e-mail: GHarvey@TycoTelecom.com; HLi@TycoTelecom.com).

Y. Hibino and S. Suzuki are with NTT Photonics Laboratories, NTT Corporation, Atsugi, Kanagawa, Japan (e-mail: yhibino@aecl.ntt.co.jp; ssuzuki@aecl.ntt.co.jp).

K.-Y. Wu is with Chorum Technologies, Richardson, TX 75081 USA (e-mail: kuangyi@chorumtech.com).

P. Xie is with Neophotonics, San Jose, CA 95134 USA (e-mail: pxie@neophotonics.com).

Digital Object Identifier 10.1109/JLT.2003.822832

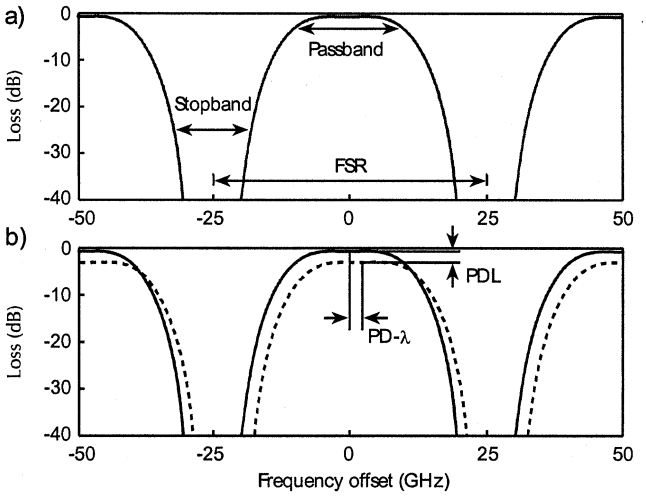

Fig. 2. Narrow-band design parameters based on output of one port from a 1:2 interleaver. (a) Output has a passband and stopband and is periodic with free-spectral range (FSR). (b) Polarization dependencies: polarization dependent loss (PDL) and polarization-dependent wavelength shift (PD-λ).

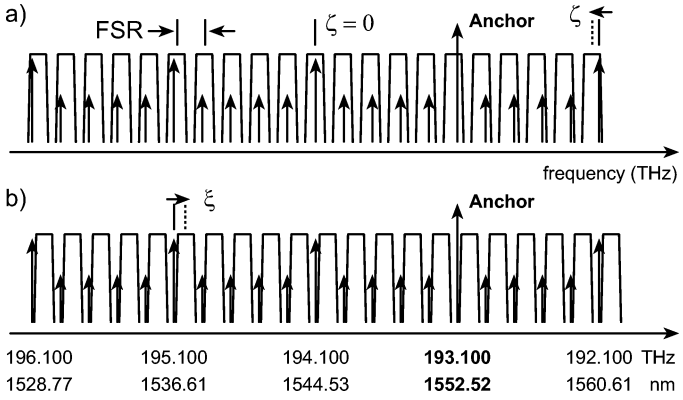

Fig. 3. Wide-band design parameters based on output of one port from a 1:2 interleaver. Arrows indicate ITU-compliant comb of 100 GHz channel spacing with anchor frequency at 193.1 THz. (a) Error of FSR produces filter walkoff over intended bandwidth. (b) Frequency-offset error (for matched FSR) misaligns all channels over the bandwidth.

polarization dependencies, Fig. 2(b), polarization-dependent wavelength (PD-λ) specifies the degree of frequency shift between s and p states and polarization-dependent loss (PDL) specifies the differential insertion loss. A third polarization parameter is the polarization-mode dispersion (PMD) which in many cases is simply differential group delay between two paths. Reduction of these polarization-dependent parameters are goals of any design.

On a wideband level there are specifications that relate to the alignment between the comb of DWDM frequencies (nominally allocated on the ITU grid [1]) and the filter function of the interleaver. The ITU recommendation specifies 100-GHz channel separation with an anchor at 193.1 THz. Many transmission systems today insert channels every 50 GHz. When the free-spectral range (FSR) of the interleaving filter is not accurately matched to the ITU grid there is walkoff, Fig. 3(a). The operational bandwidth of the filter (as opposed to the passband bandwidth) and the walkoff tolerance on the edge channels determines the allowable FSR error. For example, a 40-nm bandwidth on the C-band covers about 2.1% of the optical spectrum, and a 50-nm bandwidth on the L-band covers about 2.6%. Combination with no deadband requires 5.2% spectral coverage. The FSR must be accurate to within a channel-location tolerance (e.g., $+/-2.5$ GHz) over the appropriate spectral coverage.

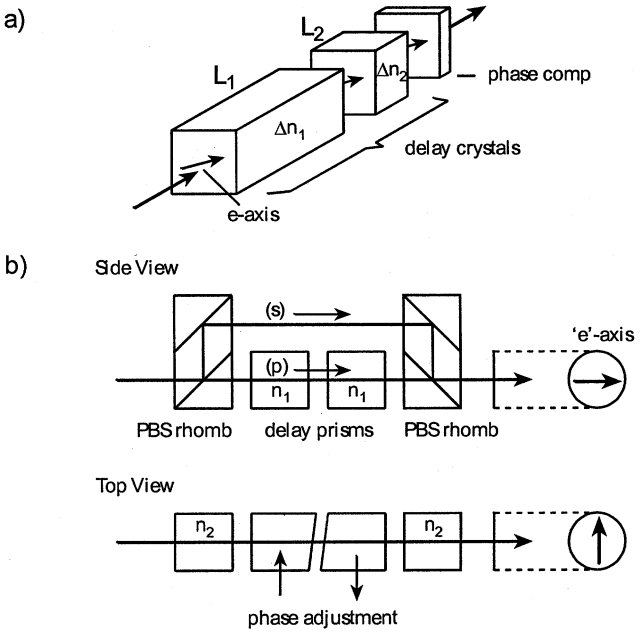

Fig. 4. Lattice filter unit cell technologies. (a) Complimentary birefringent crystals impart differential delay on orthogonal polarization states. A crystal pair is used to passively temperature compensate the birefringent phase. The phase compensation plate makes fine adjustment onto the ITU grid. The e-axes are aligned within a unit cell and cut at an angle determined by the filter synthesis. (b) Differential delay is imparted on orthogonal polarization states by an all-glass unit cell. The leading and following PBS rhombs separate the polarizations and the delay prisms determine the delay and phase.

When the FSR is matched to the ITU grid there still may be offset error, Fig. 3(b), where there is a frequency error between the centers of the interleaver channels. This frequency error is also called phase error because of the periodicity of the channels. Thermal dependence of the interleaver is the leading cause of offset error.

Cognizance of the aforementioned design goals is the background on which to understand the challenges and appreciate the remedies characteristic of the various technology solutions.

II. Interleaver Technology Approaches

There are three broad classes of interleaver filter technologies: lattice filter (LF), Gires-Tournois (GT)-based Michelson interferometer, and arrayed-waveguide router (AWG). Within the lattice filter class there is the birefringent filter, employing birefringent crystals and classically known as a Lyot or Solc filter; the glass-based filter which substitutes an artificial polarization-dependent delay for the birefringent elements of the preceding type; and the Mach-Zehnder filter, which is the analog to the Lyot filter and is generally made with planar waveguides. Within the GT class there is the interference filter and the birefringent analog (B-GT). Arrayed-waveguide routers have designs for single-channel and banded filters.

Lattice filters are typically used for 1:2 interleavers and can be cascaded to realize $1:2^{\mathrm{N}}$ filters. However, $2^{\mathrm{N}}-1$ interleavers are required to produce 2^{N} separate outputs, making such a design less economic. Lattice filters are also used for banded applications. The GT and B-GT filters are suitable for 1:2 interleavers and asymmetric interleavers as well. The AWG filters are well suited for $1:2^{\mathrm{N}}$ interleaving and deinterleaving in a single stage.

A. Lattice Filters

Lattice filters are made from a cascade of differential-delay elements where the differential-delay of each element is an integral multiple of a unit delay and power is exchanged across paths between the elements. The topic of lattice filter synthesis is broad and not limited to the optical domain. A general, technology-agnostic synthesis approach using Z-transforms is found in [2], [3]. Particular to optical filters, the classic synthesis papers include [4]–[7].

There are three issues to address in the study of lattice filters: the realization of the unit cell that generates the differential delay; the number of unit cells and associated intermediate power exchange; and the cascade of multiple filters to mitigate chromatic dispersion. The following lattice filter categories are distinguished by the technology of the unit cell.

1) Birefringent: The canonical birefringent filter, also known as the Lyot [9] or Solc filter [10], is constructed from a cascade of birefringent waveplates placed between two polarizers. The waveplates impart a frequency-dependent transformation on the fixed input polarization state, and the transformation is converted to an intensity profile by the output analyzer. The filter spectrum is periodic due to the intrinsic periodicity of the waveplates. A high-contrast filter employs waveplates whose thicknesses are integral multiples of a unit thickness, the free-spectral range being set by the thinnest waveplate. The degrees of freedom available to synthesize a particular filter function are the number of waveplates in the cascade, the sequence of waveplate thicknesses, the relative orientation of the extraordinary axes, and the orientation of the polarizers with respect to the waveplates.

Telecommunications applications require polarization insensitivity. Birefringent filters are adapted to these applications through polarization diversity. A polarization diversity scheme polarizes and spatially separates the input light to form two distinct and orthogonally polarized rays that are in turn passed through the waveplate cascade. After the cascade the polarizations are recombined onto two output ports. In this way, the light that would have been clipped by the output polarizer of the canonical birefringent filter is instead redirected to a complimentary port. Carlsen and Buhrer seem to be the first to apply polarization diversity to a birefringent filter by demonstrating a pair of polarization-splitting rhombs [11], [12]. Alternative schemes for passive filtering or switchable routing use birefringent beam walk-off blocks [13]–[19] and Wollaston prisms [20], [21].

The unit cell of a birefringent filter, illustrated in Fig. 2(a), is composed of three crystals forming two logical sections. One section is the differential delay, where one polarization is delayed along the slow axes of the crystals while the other is not. The other section is the phase compensation plate which fine tunes the filter fringes to the ITU grid. The phase compensation plate is usually made of crystalline quartz for its low birefringence. The extraordinary axes are aligned or crossed, and the tilt with respect to the aperture is set by the filter design. The FSR of the two-crystal delay section is

$$\mathrm{FSR} = \frac{c}{\Delta n_1 L_1 \pm \Delta n_2 L_2} \tag{1}$$

where c is the speed of light, $\Delta n_{1,2}$ is the (group) birefringence of the associated crystal, and $L_{1,2}$ is the respective crystal length. The birefringence Δn is a signed quantity, positive for positive uniaxial crystals and negative otherwise. The $+/-$ sign denotes alignment $(+)$ or crossing $(-)$ of the extraordinary axes. A useful unit for the speed of light is $c = 299.79\ \mathrm{mm} - \mathrm{GHz}$. To minimize the crystal lengths a high birefringent crystal is preferred, for example rutile or yttrium orthovanadate $(\mathrm{YVO_4})$. As reported in the product literature, the birefringence of $\mathrm{YVO_4}$ at 1550 nm is $\Delta n = 0.2039$, although batch-to-batch uniformity can be $+/-0.01$. Using $\mathrm{YVO_4}$ alone, an FSR of 50 GHz requires a length of $\sim$24.4 mm.

A central issue of the birefringent crystal is its temperature dependent retardation. The temperature dependence of $\mathrm{YVO_4}$ birefringence has been measured by one of the authors at $-27 \times 10^{-6}/^{\circ}\mathrm{C}$. At 50 GHz FSR, room temperature, and a frequency of 194.1 THz there are 3882 birefringent beats in the crystal. Over the full temperature range (-5 to $+70\ ^{\circ}\mathrm{C}$) there is a change of $+/-4$ birefringent beats. Use of $\mathrm{YVO_4}$ alone as the delay crystal would make the output filter fringes shift a total of eight FSRs over temperature. This is an unacceptable shift for the filter.

To mitigate first-order temperature dependence, two complimentary birefringent crystals are used in the unit cell. A materials pair in commercial use is $\mathrm{YVO_4}$ and $\mathrm{LiNbO_3}$. The ratio of crystal lengths determines the combined temperature dependence and the total length determines the FSR. Zero first-order temperature dependence can be achieved with a total length of $\sim$34.3 mm and a length ratio of $\sim 6.5\ \mathrm{YVO_4/LiNbO_3}$. However, there is a small quadratic remainder to the combined temperature coefficient that limits the stabilization over a very wide temperature range.

The need for the phase compensation plate comes from the difficulty to polish the delay crystals to a sub-micron precision. The birefringent beat length in a crystal is the length over which the e- and o-rays slip one full wave. The beat length for $\mathrm{YVO_4}$ is $\sim 7\ \mu\mathrm{m}$. Given that the practical length tolerance on a long crystal is $+/-3\ \mu\mathrm{m}$, the birefringent phase of any crystal is random over nearly a full beat. When a single unit cell is placed between crossed polarizers, change of the birefringent phase imparts a frequency shift of the output intensity spectrum. As a design rule, the birefringent phase of each unit cell in the cascade must be the same, and the phase must further be adjusted to align the filter to the ITU grid.

2) Glass-Delay: The glass-delay unit cell [22], [23], Fig. 2(b), is a substitute for the birefringent unit cell. An artificial polarization-dependent delay is created with glass blocks in place of the natural birefringence of crystalline materials.

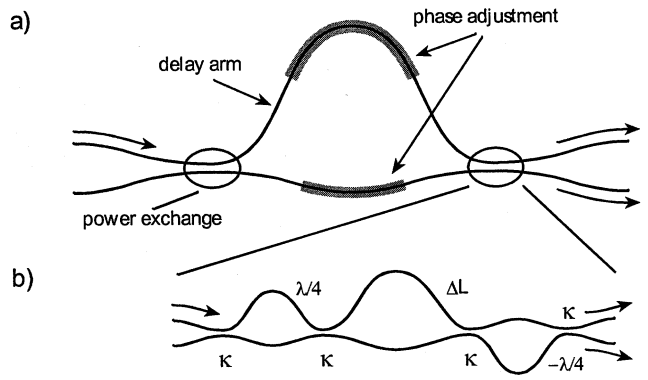

Fig. 5. The Mach-Zehnder unit cell consists of planar waveguides. (a) The path-length difference of the arms between the power couplers imparts differential delay. The heating pads adjust the phase permanently. (b) Power coupler structure for relaxing the fabrication tolerance. Cascade of four couplers with equal coupling ratios and three appropriately designed delays transfers coupling dependence from fabrication-sensitive κ to fabrication-insensitive ΔL.

The advantages are that a higher "birefringence," or differential-delay per unit length, can be achieved; the temperature characteristics of the glass materials are more linear than their crystal counterparts; and the thermal expansion of the glass materials is better matched to the hermetic housing materials.

As illustrated, the glass-delay unit cell is made with two polarization beam splitting (PBS) rhombs on either end and an glass-prism pair loaded in one of the two arms. To realize a high-quality unit cell the thin-film coatings on the PBS rhombs must produce low PDL ($<$0.1 dB) and exhibit high contrast ($>$35 dB) over a wide band ($+/-$20 nm or more). The differential delay comes from the different nL products on the two paths. The thermal dependence is mitigated by judicious selection of indices, thermal dependencies, and dimensions. As most all passive components are hermitically sealed to satisfy GR-1221 qualification requirements [24], the air-gaps in the unit cell should not experience phase drift that would otherwise be due to humidity or pressure changes [25]. To synthesize a filter function, several glass-delay unit cells are placed in cascade and each cell is rotated along the optical-transmission axis to impart the necessary power exchange.

3) Mach-Zehnder: The cascaded Mach-Zehnder (MZ) filter [26], [27], based on planar waveguide technologies [28], is the isotropic analog to the birefringent filter; the MZ filter has a lattice structure with interferometric unit cells but the birefringent filter has one with birefringent unit cells. The unit cell, Fig. 5(a), imparts differential delay between two parts by making one path longer than the other. Since the effective index of the waveguide is well controlled by the deposition process and the path lengths are well controlled by printing from a master photolithographic mask, the differential delay and associated FSR can be well aligned to the ITU grid. Final phase adjustment is done permanently with thermal-optic heating pads located above the two interferometer arms [29].

Unlike the preceding bulk technologies, active temperature stabilization is required to remain locked to the ITU grid over operational temperature, but as this is the same requirement for AWGs the increment cost for the temperature control on a multifunction chip is marginal.

The interleaver uses directional couplers to set the power ratio between the MZ unit cells. However the coupling ratio based on a simple directional coupler is sensitive to fabrication variations such as the waveguide gap and waveguide width. This sensitivity results in serious performance degradation of the filter. On the other hand, the planar waveguide technologies have features such as highly accurate waveguide delay lengths and good uniformity of coupling ratios for like couplers in a small area. Taking advantage of these features, the novel coupler structure shown in Fig. 5(b) was developed for stabilizing the coupling ratio [30]. This coupler has four individual directional couplers and three wavelength order delay parts. The delay values of the two ends are set at $\lambda/4$ and $-\lambda/4$, and the center value is set at between 0 and $\lambda/2$ depending on the desired coupling ratio. These values are so small that the two waveguides in these delay sections can be located close together. Consequently, these wavelength-order delay sections are very stable with respect to fabrication conditions. The total coupling ratio η of the circuit as a function of the individual coupling ratio (κ) is

$$\eta = (8\kappa - 24\kappa^2 + 32\kappa^3 - 16\kappa^4)\cos^2\left(\frac{\pi\Delta L}{\lambda}\right) \qquad (2)$$

when $\Delta L = \lambda/6$ and $\kappa \sim 50\%$, the total coupling ratio is 50%. Even if the κ value varies in manufacturing between 30$\sim$70%, the η value is stabilized within 48 $\sim$50%. This means this novel coupler structure has relaxed fabrication tolerances on the coupling ratio κ. By designing appropriate ΔL values, the desired coupling ratio η can be realized with a wide κ tolerance. The proposed coupler compensates well for the deviation caused by fabrication error and polarization dependence and also reduces its wavelength dependence.

Using any of these three differential-delay unit cell types, an interleaver core can be realized. Interleaver cores used in the industry include two unit-cell filters where one unit cell is twice the length of the other (a 1:2 sequence) and three unit-cell filters having a 1:2:2 delay sequence. Since the design goal is a periodic square-wave amplitude response, which has only odd Fourier components, a sequence such as 1:3:5 cannot be used. Generally, the more unit cells the better the isolation. However, there is the obvious economic tradeoff between isolation and cost.

Due to the absence of reflections, a lattice filter in any technology can be designed to be free of chromatic dispersion because its transfer function has a finite-impulse response (FIR) and contains only zeros. By carefully choosing the zero locations one can design a pair of complimentary filters with the same amplitude response and opposite delay response.

The first demonstration of a two-stage dispersion-compensated MZ-type interleaver was by Hitachi Cable [31], [32]. There, the first- and second-stage filters are the same and the output ports of the first filter are connected to the input ports of the second filter to compensate the dispersion. As an alternative but equivalent configuration, the second-stage filters can be shifted by 1/2 FSR and the connections to the outputs from the second-stage filters are altered. This configuration can be an advantage for chip layout.

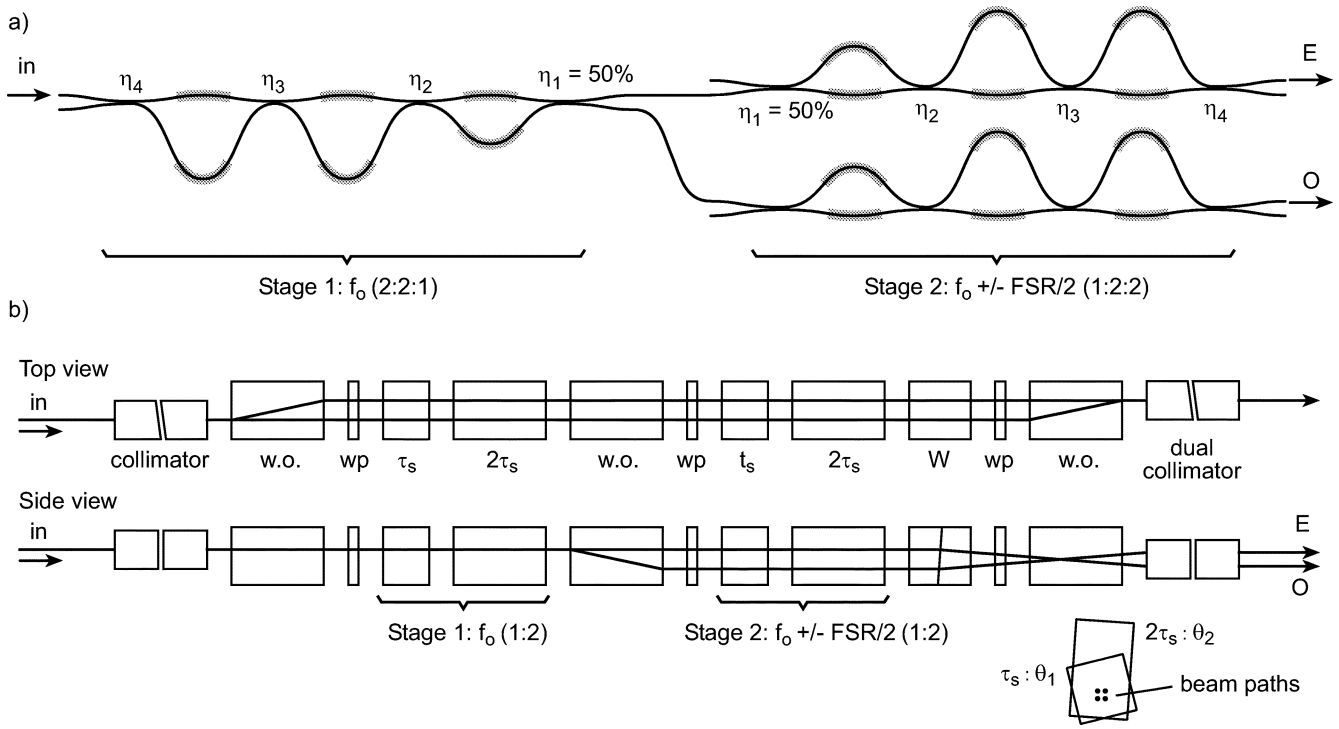

Fig. 6. Mach-Zehnder and birefringent dispersion-compensated dual-stage lattice filters. (a) Three MZ unit cells in a 1:2:2 design. The first filter has channels centered at f_o while the second pair of filters is shifted by 1/2 FSR. This design is implemented in a folded-coin layout to maximize real-estate utilization. (b) Two birefringent unit cells in a 1:2 design. The filters of the first and second stage are offset by 1/2 FSR as in the MZ design. The second stage of the birefringent filter uses path diversity to achieve two optical filters from the same physical filter. Inset shows the relation of beam paths to the cells.

Fig. 6 illustrates Mach-Zehnder and birefringent dual-stage lattice filters that compensate for chromatic dispersion. For the MZ, Fig. 6(a), the first interleaver is followed by an interleaver pair, one for each output port, where the center frequency of the pair is shifted by $+/-\mathrm{FSR}/2$. For example, in the case of a 50-GHz interleaver, the center frequencies of first and second filters are 194.10 and 194.05 THz, respectively. The interleaver pair cancels the positive dispersion on the first stage with equal negative dispersion on the second stage. This technique is employed in all commercially available lattice filters. The authors from NTT have realized this waveguide circuit using a "folded-coin" layout that fold the 200-mm path length into an area of 56×22 mm. Eight chips can be arranged in this way on a six-inch wafer. The FSR shift of the second stage was used to enable monitor waveguides to run along the folded-coin layout without any waveguide crossovers.

Fig. 6(b) illustrates one realization of a chromatic-dispersion compensated birefringent interleaver. The input and output are single- and dual-fiber collimators, respectively. As illustrated, the two interleavers are of 1:2 type, where each stage is a glass-type delay. A birefringent-crystal delay is equally suitable. The mode mixing between segments in a stage is done by physical rotation of the elements. The walk-off (w.o.) blocks together with the associated waveplates (wp) establish the polarization diversity paths that separate and later combine the polarizations. A Wollaston (W) prism is used to deflect the parallel beams into the angular aperture of the dual-fiber collimator. It should be noted that there are many folded lattice-filter designs that are designed to multiply transit the same differential delay element, reducing the cost and size of the filter [33]–[37].

For either the three-element MZ or two-element birefringent lattice, the zeros (6 and 4, respectively) of the transfer function are complimentarily arranged about the unit circle, which provides for dispersion-free design.

B. GT-Based Filters

The GT-based interleavers operate on the periodic response of a GT interferometer (GTI). Such an interleaver is configured as a Michelson interferometer where a GTI is loaded into each arm. There are two types of GT based interleavers: the interferometric type [38]–[43] that operates on the phase returned from the two Michelson arms and the birefringent type [44]–[48] that operates on the polarization returned from each arm, Fig. 7 and 8 respectively. In either case, there are two outputs for a single input and, while the illustrations show one output coincident with the input, there are usually two different collimators or a single dual-fiber collimator on the input side. This requires a small tilt of the various reflectors.

An analog of the GTI is the ring-resonator filter. In such a filter, traveling waves in the ring rather than standing waves in a GT cavity are used to generate a filter response on an evanescently coupled waveguide. These filters show promise [49], [50] and are in the development stage.

1) Interferometric: Fig. 9(a) illustrates the cavities in a glass-based GT interleaver. The GTI is constructed with a leading partially reflective mirror and a following fully reflec-

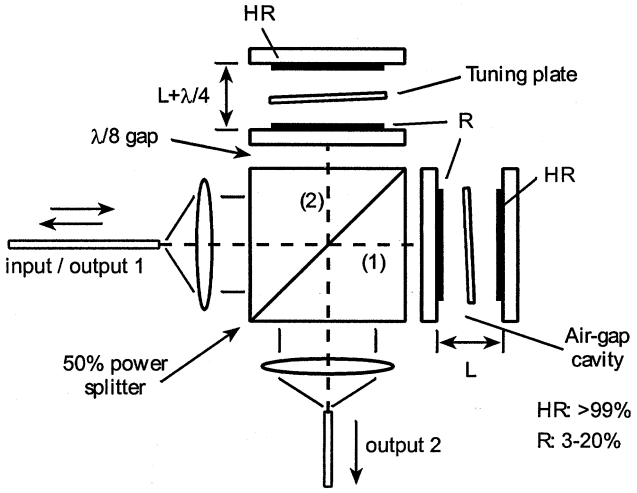

Fig. 7. Interference GT-based interleaver. A GT cavity is loaded into each arm of a Michelson interferometer, the phase difference being an eighth wave. The cavities are detuned from one another by an aggregate half-wave so one is antiresonant when the other is resonant. The tuning plates located in the air-gap cavities help tune the final filter shape. The cavity length sets the FSR of the interleaver. The 50/50 power splitter interferometrically combines the light returning from arms (1) and (2).

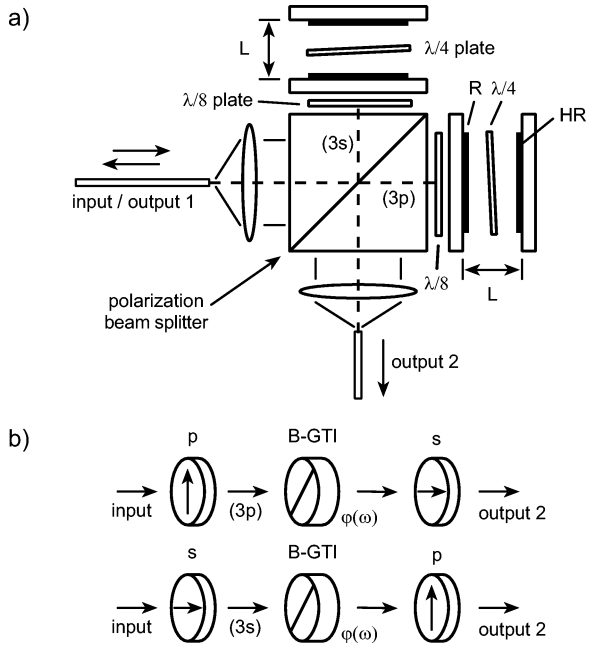

Fig. 8. Birefringent-based interleaver. (a) Similar path design to interferometric interleaver but the PBS replaces the 50/50 power splitter and waveplates set the relative retardations. The two B-GTIs are matched cavities. The frequency-dependent polarization conversion imparted from the quarter-wave plate located in the cavities is the generator of the periodic filter shape. The eighth-wave plate outside the cavity is a bias that improves the shape. (b) There is no interference on beam recombination at the PBS. Following path (3 p), the polarization is converted by the B-GTI to the right and analyzed by the PBS on return. Transmission to output 2 orients the analyzer perpendicular to the input polarizer. Path (3 s) transits the B-GTI on top with orthogonal linear polarization and is cross-analyzed by the PBS going to output 2. At output 2 the s and p polarizations passively combine.

tive mirror. The gap between mirror planes sets the FSR. The phase shift Φ_1 imparted on path (1) is

$$\Phi_1 = -2\tan^{-1}\left(\frac{1+\sqrt{R}}{1-\sqrt{R}}\tan(kL)\right) \tag{3}$$

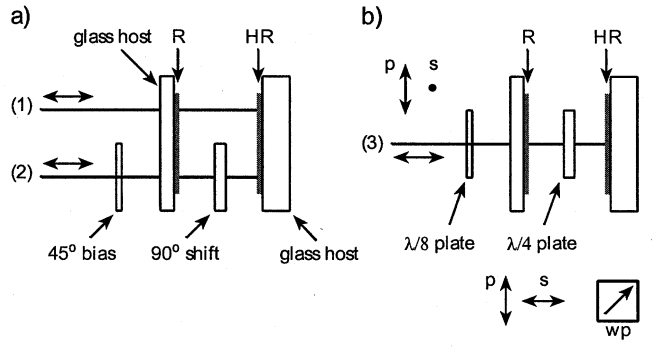

Fig. 9. Isotropic and birefringent GTIs. (a) Isotropic GTI and comparison between two paths. Gap between HR and R reflectors sets the FSR. The 90° phase shift between cavities (1) and (2) makes one resonator anti-resonant while the other is resonant. The 45° bias makes a good filter response. (b) Birefringent GTI where two paths are replaced with one, path (3), and polarizations p and s distinguish the even- and odd-channel conditions. The $\lambda/4$ waveplate (wp) inside the cavity imparts a frequency-dependent polarization conversion. The $\lambda/8$ waveplate bias makes a good filter response.

where R is the amplitude-squared reflection, k is the wavenumber, and L is the cavity length. The GTI transited by path (2) includes a quarter-wave shift inside the cavity that adds a $\pi/2$ shift to the kL product. Finally, path (2) also includes an eighth-wave shift outside of the cavity that adds a phase bias to the Michelson response. The overall phase difference between the two arms is

$$\Delta\Phi = -2\tan^{-1}\left(\frac{1+\sqrt{R}}{1-\sqrt{R}}\tan(kL)\right) + 2\tan^{-1}\left(\frac{1+\sqrt{R}}{1-\sqrt{R}}\tan\left(kL+\frac{\pi}{2}\right)\right) - \frac{\pi}{2}. \tag{4}$$

The $\pi/2$ phase shifts are themselves frequency dependent, but the phase-shift bandwidth is maximized using true zero-order shifts. Finally, the 50/50 splitting cube mixes the phase response of the two arms so that the output intensities are

$$I_1 = I_o\cos^2\left(\frac{\Delta\Phi}{2}\right), \quad I_2 = I_o\sin^2\left(\frac{\Delta\Phi}{2}\right). \tag{5}$$

A reflectivity value used by one of the authors is $R = 18\%$. Values may be tailored for a particular application.

An alternative design is to use only one GTI and make the linear delay between the two arms highly multimoded. While it may be a cost advantage to eliminate one of the resonant cavities, the path-length difference between the two arms must be tuned with an auxiliary tuning plate and the dispersion between the two arms is not matched, yielding relatively higher overall dispersion.

Temperature dependence of the cavity phase and FSR is a central challenge for the GT interleavers. Thermal-dependent index change is avoided by making cavities air-gap type. The mirrors are made from thin-film coatings deposited on glass parts, and after dicing the mirror surfaces are placed facing the inside of the cavity. Ultralow expansion materials maintain the mirror gap. Since the beat length in an air-gap cavity is the

free-space wavelength, the GT cavities must be activity aligned to achieve the right FSR. This requires submicron alignment. Moreover, the two GTI's must be activity aligned to the splitting cube to perfect the filter shape and lock the spectrum to the ITU grid.

2) Birefringent: The birefringent Gires-Tournois (B-GT) interferometer was invented in response to the tight tolerances of an isotropic GTI. In particular, for a dual-GTI interleaver, the two cavities must be out of phase by one-half wavelength. Also, the phase reference planes with respect to the splitting cube must be a quarter-wave out of phase. At 1.55 μm this requires sub-micron alignment and lifetime stabilization. However, if these two phase slips can be achieved via polarization retardation, then waveplates with a birefringent beat length of $\lambda_{\rm o}/\Delta n$ can be used. The birefringent beat length at 1.55 mm for crystalline quartz is $\sim$ 184 μm, and waveplate retardations are typically produced to within $\lambda/500$.

Fig. 9(b) illustrates a B-GT in analogy to the isotropic counterpart. Rather than two distinct paths (1) and (2), a single path with dual polarizations is used, path (3). The light impingent on the B-GT is linearly polarized by the common PBS, as illustrated in Fig. 9(b). The light first transits the bias $\lambda/8$ waveplate and then enters the B-GT cavity. The B-GT cavity is an air-gap GT with a quarter-wave waveplate added inside. The extraordinary axis is tilted 45° with respect to the TE polarization of the PBS. Ignoring the leading $\lambda/8$ plate for the moment and considering, without loss of generality, that the input linear polarization state is p, the B-GT responds on resonance by reflecting a mix of p and orthogonal s light. In anti-resonance, however, only the p state is reflected, conversion to the s state being extinguished. Adding back the bias plate, the extraordinary axis being aligned to the quarter-wave waveplate, allows filter-profile tuning. In analogy to the isotropic case, a $\lambda/8$ plate generates a balanced response.

The B-GT interleaver transforms several tolerances into polarization dependencies. The two B-GTIs must be identical. Difference in the loss translates to PDL and error in the cavity phase translates to PD-λ. Imperfections in the common PBS also contribute to polarization impairments. Difference in the path lengths between the PBS and the B-GT cavities corresponds to PMD.

GT filters have infinite impulse response and corresponding poles in the filter transfer function. Filters with poles inherently have residual chromatic dispersion. The dispersion produced by a GT interleaver can be reduced via cascading with it a second complimentary GTI. The second GTI is a single all-pass resonator with its resonance shifted by one-half FSR. The ability of the dual-stage GT to cancel dispersion depends on the Q of the resonator, or equivalently the partial reflectivity of the leading mirror. A high reflectivity sharpens the phase response and reduces the resonance bandwidth; the nonlinearity of the phase cannot be completely canceled. A low reflectivity has a more sinusoidal delay response that can better be compensated. In practice the GTI's in an interleaver core are low Q and dispersion can be limited to below 20 ps/nm for a compensated design. For a general treatment of dispersion in optical filters, see [51].

C. Arrayed-Waveguide Router Filters

The arrayed-waveplate router (AWG) is an alternative to the cascaded Mach-Zehnder lattice filter and can be designed for interleaving applications. An AWG is a generalized Mach-Zehnder, where the former has many arms that interfere at the output while the latter has only two interfering arms. Fourier filter components are produced by adding arms to the grating, each arm being monotonically longer (or shorter) than an adjacent arm by a fixed amount. Unlike a Mach-Zehnder, an AWG can have many outputs for a single input, making the AWG suitable as a single-stage $1:N$ interleaver.

The multiple waveguides between the two star couplers establish a grating. The free-spectral range of the grating is

$$\mathrm{FSR} = \frac{c}{n_g \Delta L} \tag{6}$$

where $\mathrm{n_g}$ is the group index of the waveguides at the center-channel wavelength and ΔL is the path-length difference between adjacent grating arms. The center frequency for a grating order m is simply

$$f_o^{(m)} = m\mathrm{FSR}. \tag{7}$$

The same center frequency can be reached via a large grating order and small FSR or a small grating order and large FSR.

Generally AWG's used for multiplexing applications have an FSR that covers the entire operating bandwidth. For instance, 32 nm will cover the C-band. A low grating order is correspondingly required. For interleaving applications, however, the FSR is reduced so that one in every N channels is output on the same port. In particular, the FSR is selected as

$$\mathrm{FSR} = N \times C \tag{8}$$

where C is the channel spacing. Across an operating band, such as the C-band, there are M bands each an FSR wide.

Within an FSR there are N channels and N corresponding output ports. Within a particular grating order the output waveguides are placed to accept light from each of the N channels. This requires a certain lateral separation between adjacent ports. The problem is that for different grating orders the optimal waveguide separation is different. Or, equivalently, for fixed output locations, the channel spacing within a grating order differs from order to order. The worst-case channel offset in frequency from its target frequency is [52]

$$\Delta f|_{\max} = \frac{\mathrm{M(FSR)}^2}{2\mathrm{FSR} + 4f} \tag{9}$$

For example, for an FSR of 800 GHz, 5 bands, and $f = 193.1$ THz, the worst offset is 4 GHz. This is a fundamental design tradeoff for AWG interleavers that limits the channel-spacing—bandwidth product. That is, the narrower the channel spacing, the narrower the operational bandwidth.

Passband flattening is achieved by the star-coupler and waveguide-interface design. Both physical and interferometric passband flattening schemes have been proposed and demonstrated [53]–[55]. The AWG filter is an FIR filter that has relatively low dispersion. Cascading devices to compensate dispersion is not required.

TABLE I
REPRESENTATIVE INTERLEAVER SPECIFICATIONS VERSUS TECHNOLOGY

Specification		GTI	Bulk Lattice	WG MZ	AWG	Units
Channel spacing		6.25 – 200 (50 nom.)	25 – 200 (50 nom.)	25 – 200 (50 nom.)	25 – 200 (50 nom.)	GHz
Insertion loss		0.7	1.5	2.0	5.0	dB
Pass band	-0.5 dB	+/- 16	+/- 10	+/- 11	+/- 11	GHz
	-1.0 dB	+/- 19	+/- 14	+/- 13	+/- 13	GHz
	-3.0 dB	+/- 22	+/- 17	+/- 16	+/- 16	GHz
Rejection band	-20 dB	+/- 16	+/- 18	+/- 16	+/- 16	GHz
	-25 dB	+/- 12	+/- 16	+/- 14	+/- 14	GHz
IL ripple		0.3	0.4	n/a	n/a	dB
Wavelength accuracy						
Frequency centering error		1.0	+/- 1.0	2.0	+/- 2.0	GHz
Center frequency drift over temp		2.0	+/- 2.0 (+/- 0.5 glass)	temperature stabilized	temperature stabilized	GHz
Polarization dependencies						
PDL		0.2	0.3	0.2	0.3	dB
PMD		0.2	0.2	< 2.3 (for CS=25G)	0.5	ps
PD-λ		0.5	1.0	2.1	1.0	GHz
Chromatic dispersion		+/- 80 (10 w/ comp)	+/- 15	+/- 20	+/- 20	ps/nm
Operating temperature		-5 to +70	-5 to +70	stabilization req'd	stabilization req'd	^{o}K

III. DISCUSSION

The study of interleaver technologies is particularly interesting because of the variety of successful architectures. More than 30 U.S. patents have been issued in the last five years alone. The OFC'03 Interleaver Workshop and this paper provide a snapshot of the current state-of-the-art. To this end, Table I is a compilation of specifications presented at the Workshop where each technology is individually broken out. It is always dangerous to publish specifications since technology invariable improves, but the goal is rather to mark a point in time for an overall comparison.

In terms of the variety of interleaver solutions, there is no clear technology "winner;" each technology has its unique features and its own economics. Application will ultimately determine which technology is most suitable, and different applications may require different technologies. In this sense the body of work developed to date provides a richness of choice for the system designer. Moreover, with the technological and theoretical foundations laid thus far, more sophisticated applications and denser function integration will continue to improve the economics and application breadth for interleaving filters, cementing their existence in the optical network.

ACKNOWLEDGMENT

The authors wish to thank the Optical Fiber Communication Conference organization for hosting the Workshop on interleaver technologies and the Editors of the *Journal of Lightwave Technology* for compiling this special issue.

REFERENCES

[1] *Spectral Grids for WDM Applications: DWDM Frequency Grid*, International Telecommunication Union Std. ITU-T G.694.1, June 2002.
[2] C. K. Madsen and J. H. Zhao, *Optical Filter Design and Analysis: A Signal Processing Approach*. New York: Wiley-Intersci.; Wiley, 1999.
[3] A. V. Oppenheim, R. W. Schafer, and J. R. Buck, *Discrete-Time Signal Processing*, 2nd ed. Upper Saddle River, NJ: Prentice-Hall.
[4] J. W. Evans, "The birefringent filter," *J. Opt. Soc. Amer.*, vol. 39, no. 3, pp. 229–242, 1949.
[5] S. E. Harris, E. O. Ammann, and I. C. Chang, "Optical network synthesis using birefringent crystals. I. Synthesis of lossless networks of equal-length crystals," *J. Opt. Soc. Amer.*, vol. 54, no. 10, pp. 1267–1279, 1964.
[6] A. Yariv and P. Yeh, *Optical Waves in Crystals*. New York: Wiley-Intersci.; Wiley , 2003.
[7] W. J. Rosenberg and A. M. Title, "Solc filter engineering," *SPIE Polarizers and Applications*, vol. 307, pp. 106–111, 1981.
[8] K. Jinguji and M. Oguma, "Optical half-band filters," *J. Lightwave Technol.*, vol. 18, pp. 252–259, 2000.
[9] B. Lyot, Comptes Rendus, vol. 197, p. 1593, 1933.
[10] I. Solc, Casopis prof Fysiku, vol. 3, p. 366, 1953.
[11] W. J. Carlsen and P. Melman, "Birefringent Optical Multiplexer With Flattened Bandpass," U.S. Patent 4 685 773, Aug. 11, 1987.
[12] C. F. Buhrer, "Optical Wavelength Multiplexer/Demultiplexer and Demultiplexer/Multiplexer," U.S. Patent 4 987 567, Jan. 22, 1991.
[13] K.-Y. Wu and J.-Y. Liu, "Programmable Wavelength Router," U.S. Patent 5 867 291, Feb. 2, 1999.
[14] ——, "Switchable Wavelength Router," U.S. Patent 5 912 748, Jun. 15, 1999.
[15] ——, "Programmable Wavelength Router," U.S. Patent 5 978 116, Nov. 2, 1999.
[16] ——, "Optical Wavelength Router," U.S. Patent 6 137 606, Oct. 24, 2000.
[17] ——, "Method and Apparatus for Wavelength Multiplexing/Demultiplexing," U.S. Patent 6 163 393, Dec. 19, 2000.
[18] J. N. Damask and C. R. Doerr, "Polarization Diversity for Birefringent Filters," U.S. Patent 6 252 711 B1, Jun. 26, 2001.
[19] ——, "Double-Pass Polarization Diversified Birefringent Filter," U.S. Patent 6 393 039 B1, May 21, 2002.
[20] Y. Huang and P. Xie, "Optical Polarization Beam Combiner/Splitter," U.S. Patent 6 282 025 B1, Aug. 28, 2001.
[21] ——, "Optical Polarization Beam Combiner/Splitter," U.S. Patent 6 373 631 B1, Apr. 16, 2002.
[22] P. Xie, S. Y. Wu, Y. Mao, W. Wang, R. B. Bettman, and N. Maluf, "Method and Apparatus for an Optical Filter," U.S. Patent Application 2002/0 154 845 A1, Oct. 24, 2002.
[23] P. Xie, "Optical Mux/Demux," U.S. Patent 6 373 604, Apr. 16, 2002.
[24] *Generic Reliability Assurance Requirements for Passive Optical Components*, Telcordia Technologies Std. GR-1221-CORE, 1999.
[25] G. Rakulijic, A. Kewitsch, and V. Leyva, "Diffractive Fourier Optics for Optical Communications," U.S. Patent Application 2003/0 011 769A1, Jan. 16, 2003.
[26] M. Oguma, K. Jinguji, T. Kitoh, T. Shibata, and A. Himeno, "Flat-passband interleave filter with 200 GHz channel spacing based on planar lightwave circuit-type lattice structure," *Electron. Lett.*, vol. 36, no. 15, pp. 1299–1300, 2000.
[27] K. Jinguji and M. Oguma, "Optical half-band filters," *J. Lightwave Technol.*, vol. 18, no. 2, pp. 252–259, 2000.
[28] A. Himeno, K. Kato, and T. Miya, "Silica-based planar lightwave circuits," *J. Select. Topics Quantum Electron.*, vol. 4, pp. 913–924, 1998.

[29] M. Kohtoku, T. Mizuno, T. Kitoh, M. Oguma, T. Shibata, Y. Inoue, and Y. Hibino, "Low loss and low crosstalk PLC-based interleave filter fabricated with automatic phase trimming method," in *ECOC2002 Tech. Dig.*, 2002.
[30] M. Oguma, T. Kitoh, Y. Inoue, T. Mizuno, T. Shibata, M. Kohtoku, and Y. Hibino, "Compactly folded waveguide-type interleave filter with stabilized coupler," in *OFC2002*, 2002.
[31] T. Chiba, H. Arai, K. Ohira, S. Kashimura, H. Okano, and H. Uetsuka, "Chromatic dispersion free Fourier transform-based wavelength splitter for D-WDM," in *OECC Tech. Dig.*, July 2000, paper 13B2-2.
[32] T. Chiba, H. Arai, K. Ohira, H. Nonen, H. Okano, and H. Uetsuka, "Novel architecture of wavelength interleaving filter with Fourier transform-based MZIs," in *OFC'01*, Anaheim, CA, March 2001, paper WB5.
[33] K. Tai, K.-W. Change, and J.-H. Chen, "Interleaver/deinterleavers causing little or no dispersion of optical signals," U.S. Patent 6 301 046, Oct. 9, 2001.
[34] J.-H. Chen, K.-W. Chang, K. Tai, H.-W. Mao, and Y. Yin, "Apparatus capable of operating as interleaver/deinterleavers or filter," U.S. Patent 6 333 816, Dec. 25, 2001.
[35] K.-W. Chang and K. Tai, "Double-pass folded interleaver/deinterleaver," U.S. Patent 6 335 830, Jan. 1, 2002.
[36] ——, "Single-pass folded interleaver/deinterleavers," U.S. Patent 6 337 770, Jan. 8, 2002.
[37] J. N. Damask, "Composite birefringent crystal and filter," U.S. Patent 6 577 445.
[38] S. X. F. Cao, "Nonlinear interferometer for fiber optic dense wavelength division multiplexer utilizing a phase bias element to separate wavelengths in an optical signal," U.S. Patent 6 169 604, Jan. 2, 2001.
[39] J.-H. Chen and K. Tai, "Optical signal interleaver," U.S. Patent 6 169 626, Jan. 2, 2001.
[40] S. X. F. Cao, Fiber optic dense wavelength division multiplexer with a phase differential method of wavelengths separation utilizing glass blocks and a nonlinear interferometer, Apr. 10, 2001.
[41] J.-H. Chen and K. Tai, "Optical signal interleaver/deinterleaver," U.S. Patent 6 268 951, Jul. 31, 2001.
[42] K. Tai, "Michelson phase shifter interleaver/deinterleaver," U.S. Patent 6 375 322, Aug. 14, 2001.
[43] B. Dingel and M. Izutsu, "Multifunction optical filter with a Michel-sn-Gires-Tournois interferometer for wavelength-division-multiplexed system applications," *Opt. Lett.*, vol. 23, no. 14, pp. 1099–1101, 1998.
[44] S. X. F. Cao, "Fiber optic dense wavelength division multiplexer with a phase differential method of wavelength separation utilizing a polarization beam splitter and a nonlinear interferometer," U.S. Patent 6 130 971, Oct. 10, 2000.
[45] ——, "Fiber optic dense wavelength division multiplexer with a phase differential method of wavelength separation utilizing a polarization beam splitter and a nonlinear interferometer," U.S. Patent 6 169 828, Jan. 2, 2001.
[46] ——, "Dense wavelength division multiplexer which includes a dense optical channel comb filter," U.S. Patent 6 205 270, Mar. 20, 2001.
[47] ——, "High-isolation dense wavelength division multiplexer utilizing a polarization beam splitter, non-linear interferometers and birefringent plates," U.S. Patent 6 273 129, Jul. 17, 2001.
[48] ——, "High-isolation dense wavelength division multiplexer utilizing birefringent plates and a nonlinear interferometer," U.S. Patent 6 307 677, Oct. 23, 2001.
[49] K. Oda, N. Takato, H. Toba, and K. Nosu, "A wide-band guided-wave periodic multi/demultiplexer with a ring resonator for optical fdm transmission systems," *J. Lightwave Technol.*, vol. 6, pp. 1016–1022, 1988.
[50] C. Madsen, "Efficient architectures for exactly realizing optical filters with optimum bandpass designs," *IEEE Photon. Technol. Lett.*, vol. 10, pp. 1136–1138, 1998.
[51] G. Lenz, B. J. Eggleton, C. R. Giles, C. K. Madsen, and R. E. Slusher, "Dispersive properties of optical filters for WDM systems," *IEEE J. Quantum Electron.*, vol. 34, pp. 1390–1402, 1998.
[52] C. R. Doerr, L. W. Stulz, M. Cappuzzo, L. Gomez, A. Paunsecu, E. Laskowski, S. Chandrasekhar, and L. Buhl, "2 × 2 wavelength-selective cross connect capable of switching 128 channels in sets of eight," *IEEE Photon. Technol. Lett.*, vol. 14, pp. 387–389, 2002.
[53] C. Dragone, "Planar 1 N optical multiplexer with nearly ideal response," *IEEE Photon. Technol. Lett.*, vol. 14, pp. 1545–1547, 2002.
[54] K. Okamoto and A. Sugita, "Flat spectral response arrayed-waveguide grating multiplexer with parabolic horns," *Electron. Lett.*, vol. 32, pp. 1661–1662, 1996.
[55] M. R. Amersfoort, J. B. D. Soole, H. P. Leblanc, N. C. Andreadakis, A. Rajhel, and C. Caneau, "Passband broadening of integrated arrayed waveguide filters using multimode interfernce couplers," *Electron. Lett.*, vol. 32, pp. 449–451, 1996.

S. Cao, photograph and biography not available at the time of publication.

J. Chen, photograph and biography not available at the time of publication.

J. N. Damask, photograph and biography not available at the time of publication.

C. R. Doerr, photograph and biography not available at the time of publication.

L. Guiziou, photograph and biography not available at the time of publication.

G. Harvey, photograph and biography not available at the time of publication.

Y. Hibino, photograph and biography not available at the time of publication.

H. Li, photograph and biography not available at the time of publication.

S. Suzuki, photograph and biography not available at the time of publication.

K.-Y. Wu, photograph and biography not available at the time of publication.

P. Xie, photograph and biography not available at the time of publication.